

# The CLIVAR C20C project: selected twentieth century climate events

A. A. Scaife · F. Kucharski · C. K. Folland · J. Kinter · S. Brönnimann · D. Fereday · A. M. Fischer · S. Grainger · E. K. Jin · I. S. Kang · J. R. Knight · S. Kusunoki · N. C. Lau · M. J. Nath · T. Nakaegawa · P. Pegion · S. Schubert · P. Sporyshev · J. Syktus · J. H. Yoon · N. Zeng · T. Zhou

Received: 1 April 2008 / Accepted: 23 July 2008  
© UK government 2008

**Abstract** We use a simple methodology to test whether a set of atmospheric climate models with prescribed radiative forcings and ocean surface conditions can reproduce twentieth century climate variability. Globally, rapid land surface warming since the 1970s is reproduced by some models but others warm too slowly. In the tropics, air-sea coupling allows models to reproduce the Southern Oscillation but its strength varies between models. We find a strong relationship between the Southern Oscillation in global temperature and the rate of global warming, which could in principle be used to identify models with realistic climate sensitivity. This relationship and a weak response to ENSO suggests weak sensitivity to changes in sea surface temperature in some of the models used here. In the tropics, most models reproduce part of the observed Sahel

drought. In the extratropics, models do not reproduce the observed increase in the North Atlantic Oscillation in response to forcings, through internal variability, or as a combination of both.

**Keywords** CLIVAR Climate of the twentieth century project · Climate sensitivity · Southern Oscillation · Sahel rainfall · North Atlantic Oscillation · Atmospheric models · Model evaluation · Regional climate

## 1 Introduction

Testing models against observed climate variability is an important prerequisite to using them to simulate the future, especially on regional scales relevant to the impacts of

---

A. A. Scaife (✉) · C. K. Folland · D. Fereday · J. R. Knight  
Hadley Centre, Met Office, Exeter, UK  
e-mail: adam.scaife@metoffice.gov.uk

F. Kucharski  
The Abdus Salam International Centre for Theoretical Physics,  
Earth System Physics Section, Trieste, Italy

J. Kinter · E. K. Jin  
Centre for Ocean-Land-Atmosphere studies and George Mason  
University, Fairfax, VA, USA

S. Brönnimann · A. M. Fischer  
Institute for Atmospheric and Climate Science, ETH, Zurich,  
Switzerland

S. Grainger  
Centre for Australian Weather and Climate Research,  
Melbourne, Australia

I. S. Kang  
School of Earth Environmental Sciences,  
Seoul National University, Seoul, South Korea

S. Kusunoki · T. Nakaegawa  
Meteorological Research Institute, Japan Meteorological  
Agency, Tokyo, Japan

N. C. Lau · M. J. Nath  
Geophysical Fluid Dynamics Laboratory, Princeton, NJ, USA

P. Pegion · S. Schubert  
NASA Goddard Space Flight Centre, Greenbelt, MD, USA

P. Sporyshev  
Voeikov Main Geophysical Observatory, St. Petersburg, Russia

J. Syktus  
Queensland Climate Change Centre of Excellence,  
Queensland, Australia

J. H. Yoon · N. Zeng  
University of Maryland, Baltimore, MD, USA

T. Zhou  
LASG, Institute of Atmospheric Sciences, Beijing, China

climate change. Models used in comparisons for the Intergovernmental Panel on Climate Change (Solomon et al. 2007) require fully coupled ocean–atmosphere formulation to predict the future transient response to anthropogenic forcing. However, coupled models contain large signals from internal variability of the ocean and inevitably contain some oceanic model errors. It is therefore difficult to test coupled models against actual twentieth century events, and where they can be tested it is difficult to ascertain whether any remaining errors are contained in the atmosphere or ocean components of the model. These limitations motivate the CLIVAR Climate of the twentieth century project experiments (Folland et al. 2002, <http://grads.iges.org/c20c>) which partially or completely specify the ocean state to better investigate whether twentieth century events can be reproduced in models. By specifying both the ocean state according to observations, and including various natural and anthropogenic forcings, we include both the immediate atmospheric effects and the feedbacks from the ocean in a manner consistent with observed twentieth century changes (c.f. Sexton et al. 2001). Nevertheless, there are potential limitations to this approach. In particular, it could be that atmosphere–ocean coupling is necessary to reproduce some aspects of climate variability. For this reason we also include selected results from fully coupled ocean–atmosphere experiments and partially coupled “pacemaker” experiments (e.g. Dong et al. 2006). In this case only tropical Pacific SSTs were specified and the rest of the ocean was free to evolve interactively with the model atmosphere (c.f. Alexander et al. 2002; Lau and Nath 2003; Cash et al. 2008). These show that ocean–atmosphere coupling does not alter our particular conclusions from the atmosphere only models. A further point to note is that the specified SST anomalies used here are also likely to have been driven by the atmosphere in many cases (Frankignoul and Hasselmann 1977) but this does not in itself prevent us from carrying out this useful test of models.

Although there are many potential choices of twentieth century climate variability to focus on, we first assess recent global warming rates over land. We also assess variations in the Southern Oscillation and winter North Atlantic Oscillation as the largest single sources of natural variability in the tropics and northern hemisphere extratropics. Both phenomena contribute to interannual variability of global mean temperature (Trenberth et al. 2002; Thompson et al. 2000). Analysis is also made of some prominent rainfall variations in the twentieth century as these have enormous impact on society and are a major focus of concern in climate change projections. In this study we examine changes in the west African monsoon rainfall in the Sahel region as an example of a prominent late twentieth century drought and in separate studies

(Kucharski et al. 2008; Zhou et al. 2008) we focus on past variations in monsoon rainfall.

## 2 Models and forcings

The contributing centres of the C20C project that participate in this model comparison are given in Table 1. Over 150 ensemble members are available, ranging in length from the last 50 years of the twentieth century to the period 1870–2002. The full set of forcings includes observed SSTs and sea-ice extents from the HadISST data set (Rayner et al. 2003), observed changes in carbon dioxide and sulphate aerosols, stratospheric aerosols due to volcanic eruptions, stratospheric and tropospheric ozone and solar irradiance changes. All models were run with the SST forcing and sea-ice extent, a subset also added greenhouse gases while a further subset also added selected forcings such as anthropogenic aerosol, solar variability, volcanic aerosol and land surface changes. Brief descriptions of the models and simulations can be found on the C20C web-page: (<http://www.iges.org/c20c>) and Table 1 contains a full list of the forcings included and a list of references in which the climatology of the models has been evaluated.

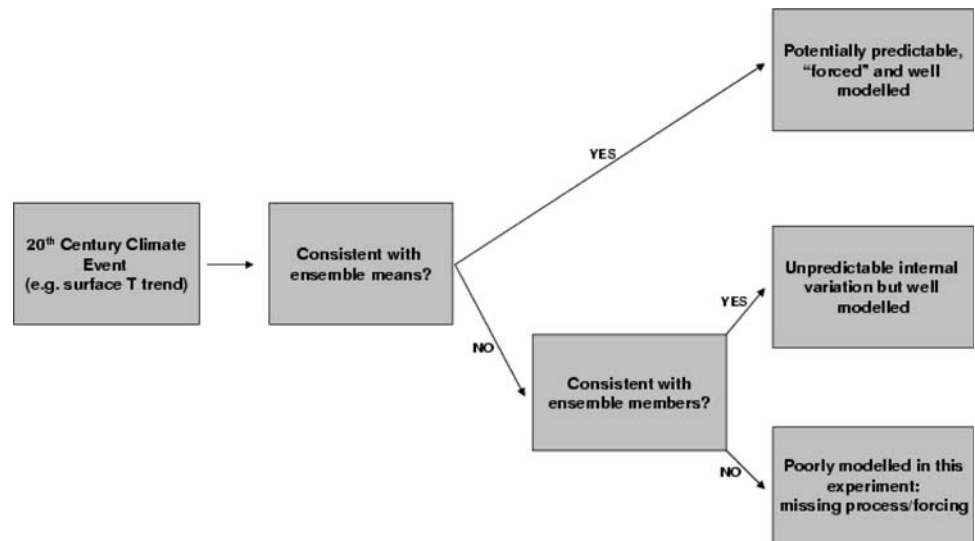
## 3 Forced and internal climate variability

A potential difficulty in deciding whether atmospheric models are capable of reproducing prominent events from the observed climate record is that the evolution of climate events may be sensitive to small atmospheric perturbations (Lorenz 1963). It is therefore probable that some prominent twentieth century events occurred due to internal atmospheric variability. By first comparing ensemble means of simulations to the observations we are able to identify which events can be reproduced given radiative forcings and observed sea surface conditions. We say that these events are “forced” even though some of the SST variability itself may be driven by the atmosphere. If the observed response is outside the range of ensemble mean model responses we compare the observations with the ensemble members to determine if the event can be said to have occurred by chance due to internal atmospheric variability. We say that these events are unforced but reproducible. Of course in reality some events may be a combination of forced and internal effects. Finally, if the observations are outside the range of both the ensemble means and the individual member ensembles we conclude that the event is poorly modelled. This process is summarised in Fig. 1.

**Table 1** CLIVAR C20C simulations of twentieth century climate

Research centre	Model	Ensemble size	Remarks	Reference
Centre for Australian Weather and Climate Research	BAM	10	SST, CO <sub>2</sub> , ozone, solar, volc	Colman et al. (2005)
Seoul National University, Korea	CES/SNU	4	SST	Lee et al. (2001, 2003)
Centre for Ocean Land Atmosphere studies, USA	NCEP	4	SST (165–290E, 10S–10N)	Saha et al. (2006)
		10	SST	
Geophysical Fluid Dynamics Laboratory, USA	GFDL	10	SST, GHG, aerosols, ozone, solar, land cover, black carbon, volc	Delworth (2006)
Hadley Centre for Climate Change, Met Office, UK	MetUM	12	SST, GHG, aerosols, ozone, solar, land cover, volc	Pope et al. (2000)
International Centre for Theoretical Physics, Italy	ICTPAGCM	10	SST	Kucharski et al. (2006)
Institute of Atmospheric Physics, LASG, China	GAMIL	3	SST, GHG, aerosols, solar	Wang et al. (2004)
Meteorological Research Institute, Japan	MRI	6	SST, CO <sub>2</sub>	Shibata et al. (1999)
NASA Goddard Space Flight Centre, USA	NSIPP	14	SST	Bacmeister et al. (2000)
		8	SST and CO <sub>2</sub>	
Queensland Climate Change Centre of Excellence, Australia	CSIRO	15	SST 1871–1948	Gordon et al. (2002)
		21	SST 1949–2003	
Uni. Maryland at College Park, USA.	CABO	9	SST, aerosol, solar, volc	Zeng et al. (1999)
Voeikov Main Geophysical Observatory, Russia	MGO	10	SST, GHG, solar, volc	Shneerov et al. (2001)
Institute for Atmospheric and climate science, ETH Zurich	SOCOL	9	SST, GHG, solar, volc, land cover, coupled ozone, QBO	Egorova et al. (2005), Schraner et al. (2008)

**Fig. 1** Analysis of modelled climate variability



#### 4 Land surface temperatures

We examine the modelled timeseries of global mean land surface air temperatures in experiments in which the sea surface temperature and ice cover is specified (Fig. 2). Increases in land surface temperature are reproduced in all models and most models show around 0.7°C increase in temperature since the middle of the twentieth century. The

observed increase in land temperatures is therefore within the range of the model ensemble means and we can conclude (Fig. 1) that the observed twentieth century warming of land surface temperatures is potentially predictable and forced (in the sense described above).

Most of the observed year-to-year fluctuations in land surface temperature are also reproduced by the models. For example, the highest observed land surface air temperature

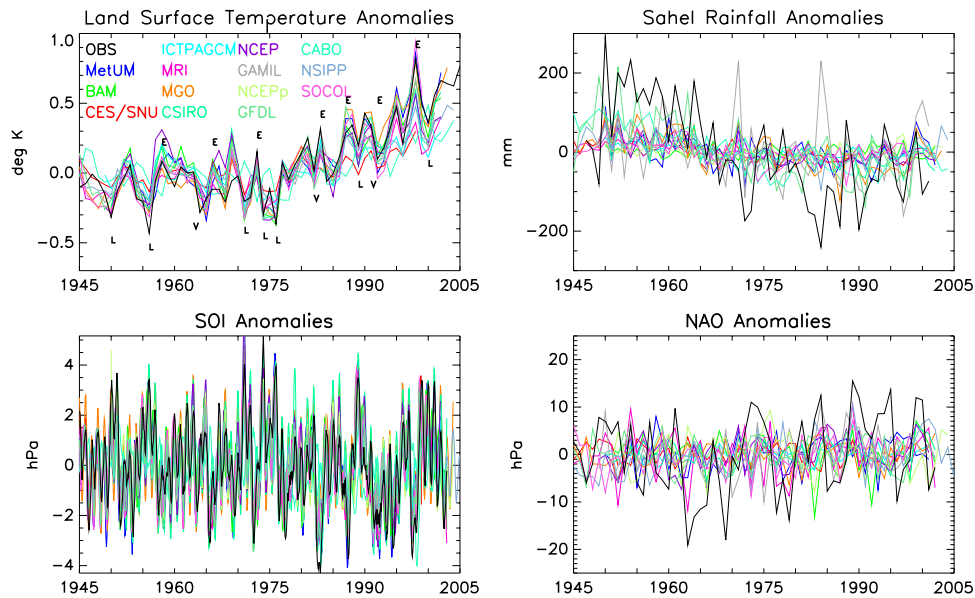


**Fig. 2** Time series of ensemble mean model simulations of: **a** Global mean land surface temperatures with large El Niño (E), La Niña (L) and volcanic eruptions (V) marked, **b** Sahel rainfall averaged over (12.5–17.5N and 15W–37.5E) and June–September, **c** Southern Oscillation index (5 month running mean PMSL difference between nearest gridpoints to Darwin and Tahiti) and **d** Winter North Atlantic Oscillation index (DJF mean of PMSL difference between nearest gridpoints to Iceland and the Azores) from 1945 to 2005. Observed

land temperatures are from CRUTEM3 (Brohan et al. 2006). Sahel rainfall data are from Hulme (1994) and GPCP data (Huffman et al. 1997) combined as in Rowell (2003). NAO and SOI indices are calculated from station data and compared to nearest gridpoint data from models. Absolute rather than normalised time series are used throughout to avoid normalising by small ensemble mean variances (c.f. Bretherton and Battisti 2000) and units are °C, mm, hPa and hPa, respectively

occurred in 1998 and a prominent peak is well reproduced by the model ensemble in this year, although some models show a much weaker peak than others. The large increase in temperature in 1998 was mainly due to the very strong El Niño event of 1997/1998. Similarly, prominent inter-annual decreases in land surface temperature during La Niña events and volcanic episodes are also reproduced. The lack of a clear decrease in land surface temperature following the eruption of the El Chichon volcano in 1982 is an exception has been noted in observations, while coupled ocean-atmosphere simulations produce a clear cooling response (Jones et al. 2007). Our simulations confirm that when the SST and hence the large El Niño event of 1982/1983 is also specified in the model, the lack of a clear decrease in land surface temperature in the early 1980s is well simulated.

The most rapid increase in observed land surface air temperatures over the twentieth century occurred in the last few decades. Observations show that since 1970, the land warmed at an accelerated rate of around 0.7°C in 30 years (Fig. 3). Trends from the models over the same period (Fig. 3) also show faster warming than in earlier periods, as indeed occurs in coupled ocean-atmosphere models simulations (Solomon et al. 2007). The range of ensemble mean modelled trends for 1970–2000 also spans the observed trend in global land temperature over that period. However, most of the models used here (8 out of

13) warm more slowly than the observed rate over 1970–2000.

It is worth noting that there were some differences in the applied variations in radiative forcings between different groups (Table 1). This could in principle explain some of the difference between the observed and ensemble mean warming rate. Three out of the five models with the weakest warming rate did not include increased greenhouse gases directly and land warming in those models arose indirectly, mainly from the imposed SST and sea-ice. While this is sufficient to generate the majority of the observed warming it slightly underestimates the actual magnitude (Sexton et al. 2001). Nevertheless, in the following section we show that an additional reason for the underestimation of near surface warming in the models is their weak response to sea surface warming in general.

## 5 The Southern Oscillation

All the models simulate a strong ocean–atmosphere coupling in the tropical Pacific and reproduce the basic characteristics of the observed variation in the Southern Oscillation index (SOI). Interannual variability in the SOI due to ENSO events is well reproduced (Fig. 2) and there is some evidence of a saturation in the surface pressure response during the strongest El Niño events (Fig. 4). This

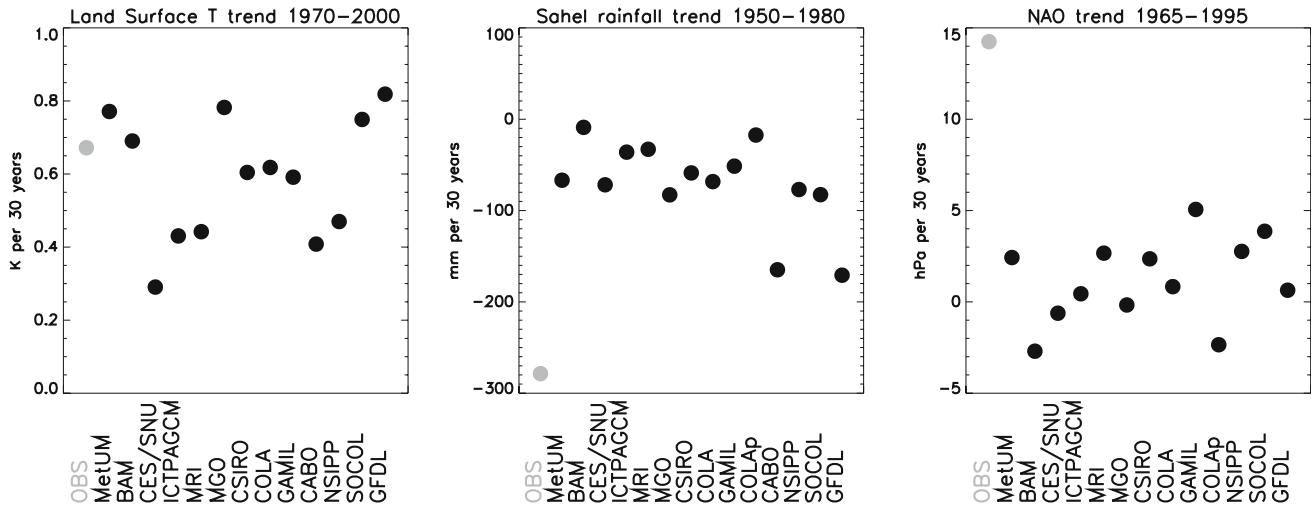


**Fig. 3** Linear trend in ensemble means for **a** Global mean land surface temperature from 1970 to 2000, **b** Sahel rainfall from 1950 to 1980 and **c** North Atlantic Oscillation index from 1965 to 1995.

Model ensemble means (*black*) and observed changes (*grey*). Changes are calculated from the linear trend and units are °C, mm and hPa, respectively

latter feature is presumably due to a full shift in the convection out to the central tropical Pacific and a corresponding complete breakdown of the Walker circulation during very strong El Niño events.

Although year to year variations in the SOI are well reproduced, there are large differences between models in the strength of the response. Figure 4 shows the modelled and observed regression coefficients between SOI and NINO3 SST. It is clear from this figure that several models underestimate the strength of the atmospheric response to ENSO. While there are many possible reasons for the variety of model responses, it is worth noting that some of

the models with the weakest response contain simplified representations of atmospheric physical processes. It is perhaps not surprising that such models show a weaker response given their limited representation of clouds and other atmospheric processes important in the Southern Oscillation. Nevertheless, even these models can show a qualitatively correct response and saturate during very strong El Niño events (not shown).

As well as the range of modelled surface pressure responses, there is also a wide variation between models in other aspects of the Southern Oscillation such as the land surface warming/cooling following El Niño/La Niña

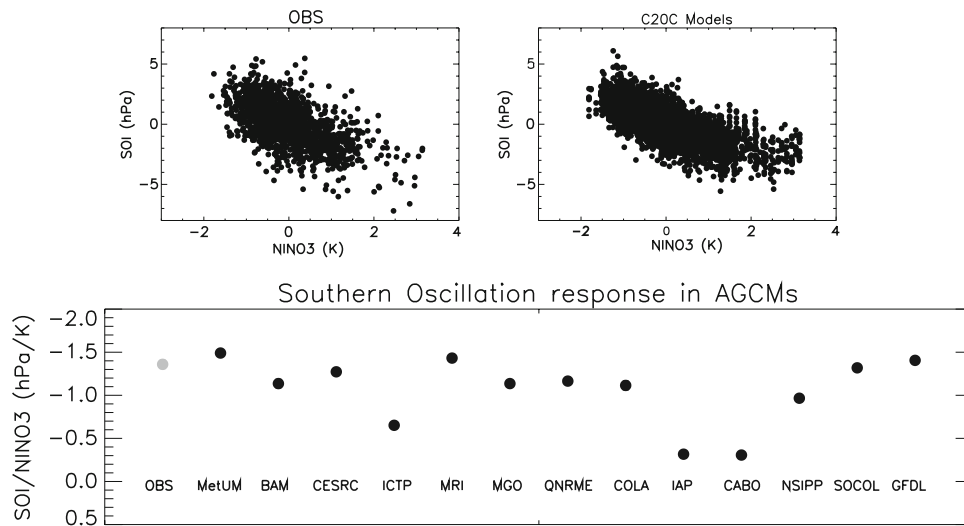


**Fig. 4** Scatter plots of monthly, deseasonalised SOI versus NINO3 (*upper*) and regression coefficients between SOI and NINO3 to measure the strength of atmospheric response to the tropical Pacific ocean (*lower*). Regression coefficients were calculated using monthly deseasonalised data. We use the point index SOI here (Tahiti-Darwin

pressure difference) as SSTs are specified and differences in the location of centres of the atmospheric response between models are therefore small. Units are hPa and °C for SOI and NINO3 index and hPa/°C for the regression coefficients

events. As shown in Fig. 2, year to year changes in observed global land temperature are often related to ENSO events. Trenberth et al. (2002) showed that global mean temperatures vary by around 0.1 K per degree change in Nino3.4 and peak a few months after the peak of the ENSO event. We therefore calculated the annual mean temperature anomaly for the year following the winter peak of ENSO events. The regression coefficient between winter Nino3 index and observed annual mean land surface temperature anomaly is 0.14K/K. Our models underestimate this sensitivity of land surface temperature to ENSO and no model produces a sensitivity as large as in the observations (see the ordinate of Fig. 5). This overall weakness of the modelled response to ENSO explains the underprediction of some of the observed interannual peaks in global land surface temperature that follow El Nino events in Fig. 2.

Comparing the strength of the ENSO response to the rate of global warming over land in recent decades reveals a very strong relationship between the amount of land surface temperature change following ENSO and the long term rate of global land surface warming in our models (Fig. 5). Models which show a weak/strong atmospheric temperature response to a given ENSO event also show weak/strong global land surface warming over the last few decades. This result also suggests that some of our models reproduce weaker warming over land than observed over the last few decades (previous section) because they respond weakly to sea surface temperature changes in general, including those from ENSO (Fig. 5).

Several studies have indicated that the strength of the global warming response in models is related to other model characteristics such as the ability of models to simulate current climate (Shukla et al. 2006), the amplitude of the ENSO cycle in the model (Toniazzi et al. 2006) or the strength of the seasonal cycle (Knutti et al. 2006). The relationship found here between the amount of annual mean land warming following a given ENSO event and the strength of the global warming rate in models could in principle change when coupled ocean–atmosphere models

rather than atmosphere only models are used so we examined the relationship in twentieth century simulations from various realisations of the HadCM3 Met Office Hadley Centre coupled ocean–atmosphere model (MetUM). These models have a range of internal parameter settings to sample model uncertainty (Murphy et al. 2007). The same relationship between land warming due to ENSO and the rate of global land warming was found in these coupled models as in the atmosphere only models. Because past warming rates are a good indicator of future warming rates in models (Stott and Kettleborough 2002) this relationship could be used to identify those climate models with more realistic climate change.

## 6 Sahel drought

The North American “Dustbowl” drought of the 1930s has already been shown to be reproducible given specified sea surface temperatures (Schubert et al. 2004). A second prominent drought period of the twentieth century is the large decrease in Sahel rainfall from the middle of the century (Folland et al. 1986). The rainfall has only partly recovered in recent years from the period of intense drought which developed from 1950 to the 1980s (Fig. 2). Figure 2 also shows that some of the observed long term decrease is reproduced by the model ensemble means. The observed year-to-year changes are not well reproduced by the ensemble means and are therefore only weakly driven by SST feedback or climate forcings. This contrasts with a study by Rowell et al. (1995) who simulated very wet and dry years with considerable skill but their model used fixed distributions of clouds unlike the models used here. The results shown here are also consistent with the large internal variability of the modelled year-to-year changes in Sahel rainfall (not shown). Although most models simulate some development of the Sahel drought between 1950 and 1980, the multimodel ensemble mean change is less than half of the observed long term change (Fig. 3). Internal

**Fig. 5** Relationship between land warming due to ENSO and transient climate warming. Regression coefficients of global land temperatures with NINO3 index are plotted against the linear rate of land surface warming over 1970–2000 for ensemble means of models (black) and observations (grey). The regression coefficients were calculated from monthly deseasonalised data and are dimensionless. The rate of land warming is in °C per 30 years

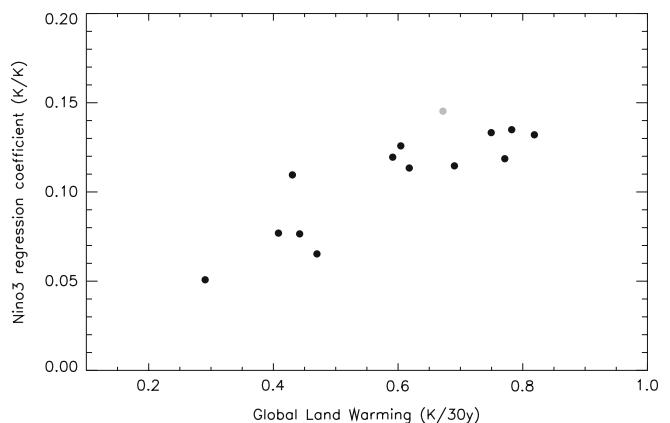
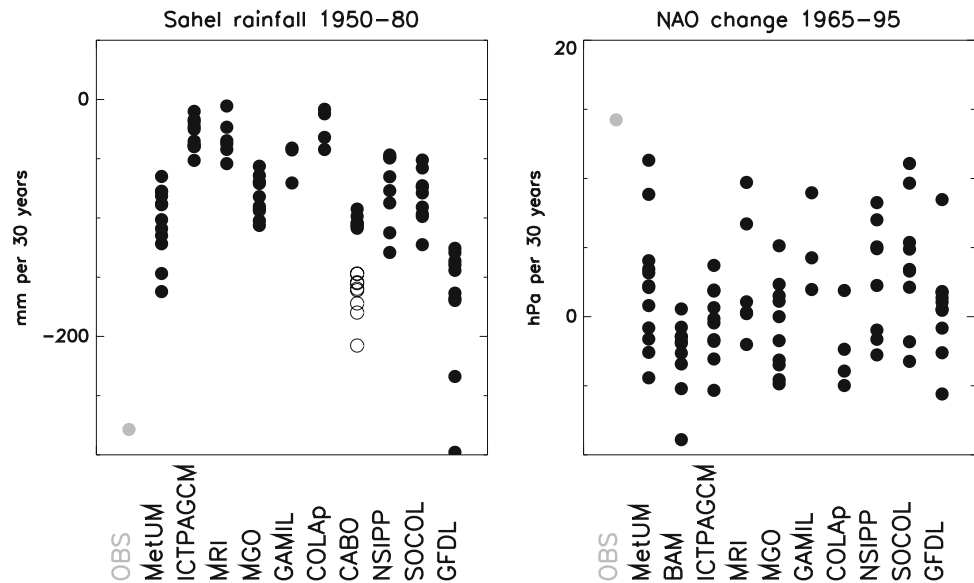


**Fig. 6** Changes in ensemble members for **a** Sahel rainfall from 1950 to 1980 and **b** North Atlantic Oscillation Index from 1965 to 1995. Model ensemble members are shown in *black* and observed changes are in *grey*. *Open circles* show the Sahel changes in simulations with interactive vegetation. Changes are calculated from the linear trend and units are mm for Sahel rainfall and hPa for the NAO



atmospheric variability is also much too small to explain the observed Sahel drought in most of the models (Fig. 6). Only the GFDL model has enough spread to explain the observed drought as a part forced and part internal variation of the climate system. Consistent with our schematic in Fig. 1, we therefore conclude that the Sahel drought is only partly forced and that it is poorly modelled in most of the models used here.

The correlation between observed Sahel rainfall and the multimodel ensemble mean rainfall over the second half of the twentieth century is 0.6; in good agreement with the single model study of Giannini et al. (2003). This suggests that around one third of the variance in Sahel rainfall can be reproduced from climate forcings and feedbacks from ocean temperatures. Figure 7 illustrates the pattern of correlation between Sahel rainfall and the sea surface temperature specified in the models. Strong correlations are found with tropical ocean temperatures, particularly in the Indian Ocean and the tropical Atlantic (c.f. Folland et al. 1986; Giannini et al. 2003). There is also a significant negative correlation with the tropical Pacific Ocean temperature that is likely to arise from ENSO (c.f. Rowell et al. 1995) and a smaller correlation with the whole Atlantic Ocean which changes sign from positive in the North Atlantic to negative in the south Atlantic. This last pattern is reminiscent of low frequency variability in the Atlantic thermohaline circulation and Atlantic SST which also affects Sahel rainfall (Zhang and Delworth 2006; Knight et al. 2006). Despite this, our multimodel study shows that the effect of sea surface temperatures alone is not sufficient to reproduce the observed drought in these model experiments and less than half of the observed drought is reproduced by the multimodel ensemble mean.

Missing processes or incorrect parametrisation of sub-grid scale processes could be responsible for the failure to reproduce the magnitude of the Sahel drought. It is interesting to note that the models which reproduce the largest change in Sahel rainfall (Fig. 3) tend to include land surface changes via parametrised vegetation-climate interaction (CABO) or specified changes (GFDL). Indeed, one of these models simulates a smaller decrease in rainfall when vegetation-climate interaction is switched off (see open circles in Fig. 6 and Zeng et al. 1999). However, there are still differences between the trends in Sahel rainfall in the different models and some of the other models show relatively weak trends despite incorporating specified vegetation changes. Therefore, although the model simulations suggest that vegetation interaction may play a role in the Sahel drought, this is sensitive to model details. Further experiments with and without vegetation feedback would be useful to confirm this result for other models. A second experiment has been run with the Hadley Centre model in which a range of interactive vegetation schemes, a coupled ocean-atmosphere model and a comprehensive set of forcings were used to try to reproduce the full magnitude of the Sahel drought. In this experiment, the interactive ocean allows sea surface temperature to vary. The spread of Sahel rainfall trends in these simulations is only slightly larger than that in the atmosphere only runs, suggesting that vegetation feedbacks on Sahel rainfall in the twentieth century are small compared to internal atmospheric variability in that model. Given the strong sensitivity in the CABO model, this again suggests that vegetation feedback on the Sahel drought is likely to be model dependent.

A second key difference between the models that produce a larger Sahel drought is the model representation of anthropogenic aerosol (Biasutti and Giannini 2006). The

GFDL and CABO models both include such aerosol which could play a direct role via atmospheric forcing. More closely coordinated experiments would be useful to determine the relative importance of aerosol and vegetation feedback although we note again that only one of our models was able to reproduce the full Sahel drought as a combination of forced and internal variability.

## 7 The North Atlantic Oscillation

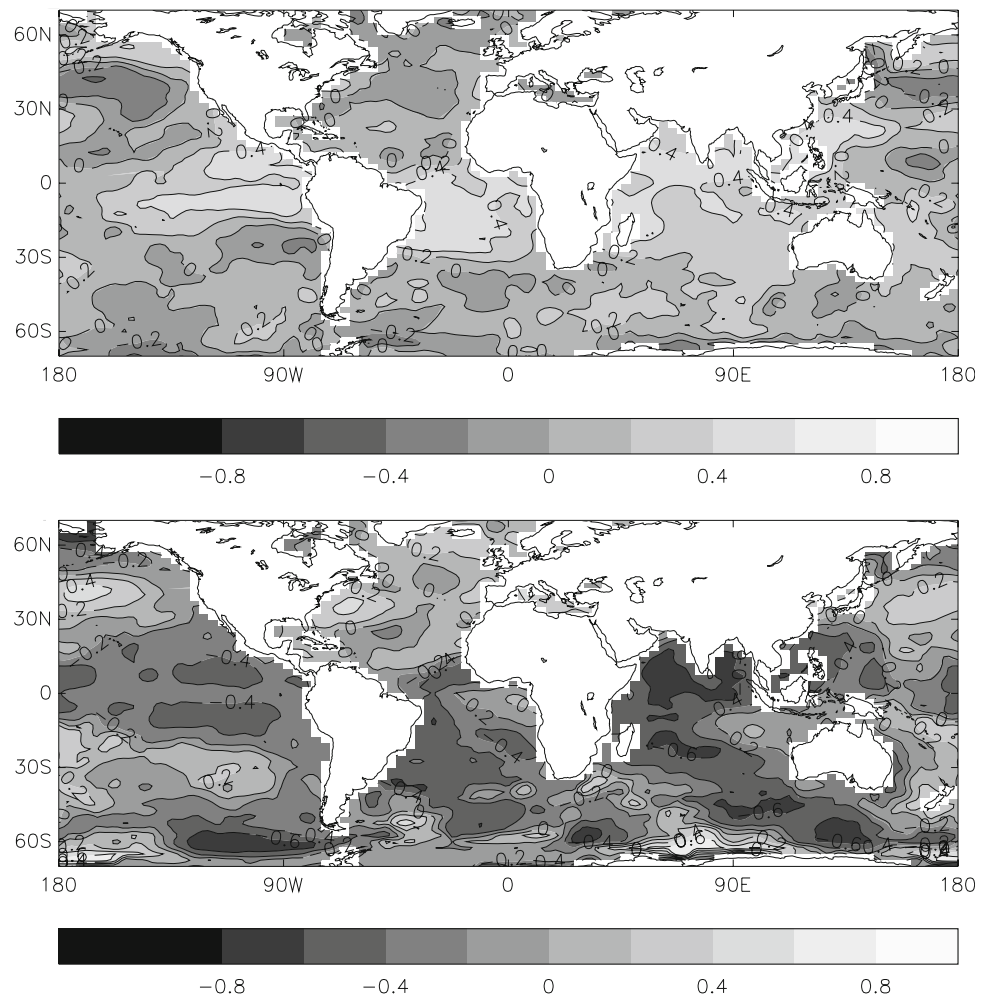
There is only very weak correspondence between the ensemble mean evolution of the NAO and the observed NAO for any of the individual models despite the prescription of observed SST and radiative forcings. Internal variability is large and dominates for small ensembles so that correlations over the latter half of the twentieth century are typically 0.1.

By taking the multimodel mean of the NAO over all our ensemble members we can remove much of this internal variability. Recent studies of similar models from the Atmospheric Model Intercomparison Project suggest no

detectable NAO response to imposed SST anomalies (e.g. Cohen et al. 2005) but with the longer data here, we find a correlation with the observed NAO of 0.3 which is significant at the 95% level. This multimodel result is similar but smaller than the correlation between modelled and observed NAO found by Rodwell et al. (1999) or Mehta et al. (2000). It suggests that the NAO is weakly forced by the imposed SST and radiative forcings in the models. The relationship between the multimodel mean NAO in the model and the imposed sea surface temperature is shown in Fig. 7. The general North-to-South pattern of negative–positive–negative Atlantic sea surface temperature anomalies associated with the positive NAO in observations (Namias 1964; Ratcliffe and Murray 1970; Palmer and Sun 1985; Rodwell et al 1999) is hardly visible here and this suggests that North Atlantic conditions feed back only weakly onto the NAO in these models.

Assuming our models are realistic, the feedback between ocean surface conditions and the NAO is responsible for less than 10 percent of the observed variance in the NAO. Despite this, the response of the atmosphere to midlatitude sea surface temperature appears

**Fig. 7** Correlation coefficients between the sea surface temperatures and multimodel ensemble mean Sahel rainfall (*upper*) and NAO index (*lower*). Values above 0.25 are statistically significant at the 95% level



to be stronger in nature (Rodwell and Folland 2002; Rodwell et al. 2004) and the weak model response may be due to lack of horizontal resolution (c.f. Nakamura et al. 2005). Model experiments with resolution of a few tens of km may be needed to resolve this issue (Maloney and Chelton 2006; Minobe et al. 2008). The poor reproduction of observed year to year NAO variations by the ensemble mean is also likely to be degraded by the potential influence of volcanic events and ENSO on the NAO. Volcanic aerosol was not included in all the simulations shown here. Besides which, the tendency for positive NAO conditions to appear after explosive tropical eruptions is not well represented in at least some of the models (Stenchikov et al. 2006). Similarly, the remote effects of ENSO on the NAO are also not well represented in at least in some of the models here (Toniazzo and Scaife 2006). Figure 7 shows that correlations between ENSO and the multimodel mean NAO is positive in these experiments whereas the observed relationship is negative (e.g. Bronnimann 2007).

On longer timescales, a major twentieth century event was the sharp rise in the winter NAO over the 1965–1995 period followed by a subsequent decrease. The multimodel mean NAO shows some increase over the 1960s–1990s period but with trends from individual models distributed about zero (Fig. 3). Some authors have argued that low frequency warming of the tropical oceans, and in particular the Indian Ocean is responsible for the observed NAO increase over the latter half of the twentieth century (Hoerling et al. 2001, 2004; Hurrell et al. 2004; Bader and Latif 2005). We find some evidence for this as tropical sea surface temperatures, including those in the Indian Ocean are positively correlated with our multimodel mean NAO. Interestingly we also find strong correlations with the tropical Atlantic. However, while a positive NAO was simulated in response to tropical ocean warming in our simulations, the magnitude of the modelled change was still much weaker than the observed change (Fig. 3) and over the last 10 years the NAO has decreased while the observed Indian Ocean warming continued. This is consistent with the model study by Schneider et al. (2003) who also found that the observed magnitude of circulation trends over the Atlantic were not reproduced in response to ocean forcing. In fact this also agrees with the model response found by Hoerling et al. (2001) which was more than a factor of 2 weaker than the observed change over the period 1950–1999 and weaker still over the period considered here. Similarly, Bader and Latif (2005) applied an idealised Indian Ocean SST anomaly which was much larger than the observed Indian Ocean change to produce a model response which was smaller than the observed change in the NAO. It therefore seems that the C20C simulations presented here are in agreement with these earlier studies in simulating a weak positive shift in the

NAO in response to observed sea surface temperature change and this response is much smaller than the observed NAO increase.

As the NAO responds only weakly on these multidecadal timescales, in line with the schematic in Fig. 1 we compared the observed increase over the latter part of the twentieth century with the individual ensemble members (Fig. 6). Neither ensemble spread, nor intermodel differences can easily explain the observed increase in the NAO over 1965–1995. We also examined 30 year NAO trends in the ensemble members over other periods in the late twentieth century in order to better assess whether internal variability could generate the observed trend. We found that the observed 30 year trend could not be reproduced in over 3700 years of model data. We conclude that the observed increase of the NAO is not reproduced in these models and that there may be a missing process or a missing forcing that amplified the NAO increase. One candidate for this missing process is the interaction with the stratosphere. Observed stratospheric change and the strength of stratosphere-troposphere coupling are known to be large enough to reproduce the observed increase in the NAO (Scaife et al. 2005). It is therefore perhaps not surprising that the models used here do not simulate the observed NAO increase over this period as their stratospheric resolution is generally low. It is also interesting to note that one of the models, which has a more detailed representation of stratospheric processes than the other models (including full interactive chemistry), exhibits the second largest NAO trend in the ensemble mean (SOCOL model, Fig. 3).

## 8 Discussion and conclusions

One aim of the CLIVAR Climate of the twentieth Century project (Folland et al. 2002) is to test whether models are able to reproduce recent climate variations and to find the mechanisms responsible. Unlike coupled ocean–atmosphere model simulations such as those used by the Intergovernmental Panel on Climate Change, these simulations specify ocean surface conditions such as sea surface temperature in part or all of the ocean and therefore capture some of the prominent interannual variations in the observational global climate record such as El Niño events.

We have used ensembles of these simulations to decide whether several recent climate events are a response to specified boundary conditions such as sea-surface temperature and/or greenhouse gases, a result of internal variability of the atmosphere, or neither, in which case we conclude the event is not well modelled. In summary we find that:

1. Global land surface temperature is generally well reproduced by atmospheric models, including

interannual and multiannual changes due to ENSO for example. However, the increase in land surface temperatures since 1970 is underestimated in many of the models used here.

2. Temporal variations in the Southern Oscillation are well simulated in atmospheric models but the strength of the Southern Oscillation response to specified SSTs varies between models. In some models the strength of the response differs significantly from that seen in observations.
3. There is a clear relationship between the strength of the global temperature response to a given ENSO event and global surface warming in the models. This could, in principle, be used to help identify models which simulate realistic climate change.
4. The Sahel drought is only weakly reproduced in most models. More drought is reproduced in models when interactive vegetation and anthropogenic aerosols are included but this result is model dependent.
5. SST and radiative forcings exert a weak influence on the North Atlantic Oscillation in the models. None of the models used here reproduces the observed increase in the NAO in the late twentieth century through forced or internal variability or a combination of both.

The results shown here highlight the importance of confronting models with observed climate variability. It is important to understand the mechanisms of climate variability and to check that these are well modelled because climate variability can severely exacerbate or temporarily alleviate long term anthropogenic climate change. Model based attribution of past events to anthropogenic forcings relies on accurate simulation of both forced and internal variability. We have shown that all models have some regions where this is not the case and caution is needed to interpret attribution of climate events in these regions. Similarly, regional climate change is uncertain in some parts of the world and the latest round of predictions shows inconsistency even in the sign of some changes. Climate prediction and attribution of past events in regions which turn out to be poorly modelled according to the schematic in Fig. 1 may still be useful on century long timescales when the effects of climate warming are likely to dominate. However, on decadal timescales such as those considered here, they are subject to the additional caveat that we are unable to fully reproduce their observed variations.

**Acknowledgments** This work contributes to the CLIVAR Climate of the twentieth Century project: <http://www.iges.org/c20c/home.html> and was carried out with support from the UK Met Office's Hadley Centre climate research program: joint Defra and MoD Programme, (Defra) GA01101 (MoD) *CBC/2B/0417 Annex C5*. We thank Dr J. Murphy for useful comments and Drs B. Booth, M. Collins and G. Harris for coupled ocean atmosphere data from the Hadley Centre model and Dr D. Rowell for the Sahel rainfall data. J. Kinter and

K. Jin were supported by research grants from NSF (0332910), NOAA (NA04OAR4310034) and NASA (NNG04GG46G). P. Sporyshev was supported by the Russian Foundation for Basic Research. S. Grainger was supported by the Australian Climate Change Science Program of the Australian Greenhouse Office. The development and maintenance of CCM SOCOL was funded by ETH Zurich grant PP-1/04-1.

## References

- Alexander MA, Bladé I, Newman M, Lanzante J, Lau N-C, Scott J (2002) The atmospheric bridge: The influence of ENSO teleconnections on air-sea interaction over the global oceans. *J Climate* 15:2205–2231
- Bacmeister JT, Pegion PJ, Schubert SD, Suarez MJ (2000) An atlas of seasonal means simulated by the NSIPP 1 atmospheric GCM. NASA Tech. Memo. 104606, Vol. 17, 194 pp. Available from Goddard Space Flight Center, Greenbelt, MD 20771
- Bader J, Latif M (2005) North Atlantic response to anomalous Indian Ocean SST in a coupled GCM. *J Clim* 18:5382–5389
- Biasutti M, Giannini A (2006) Robust Sahel drying in response to late 20th century forcings. *Geophys Res Lett* 33:L11706
- Bretherton CS and Battisti DS (2000) An interpretation of the results from atmospheric general circulation models forced by the time history of the observed sea surface temperature distribution. *Geophys Res Lett* 27:767–770
- Brohan P, Kennedy JJ, Harris I, Tett SFB, Jones PD (2006) Uncertainty estimates in regional and global observed temperature changes: a new dataset from 1850. *J Geophys Res* 111:D12106., doi:[10.1029/2005JD006548](https://doi.org/10.1029/2005JD006548)
- Bronnimann S (2007) The impact of El Niño/Southern Oscillation on European climate. *Rev Geophys* 45:RG3003
- Cash BA, Rodó X, Kinter JL III (2008) Links between tropical Pacific SST and cholera incidence in Bangladesh: role of the eastern and central tropical Pacific. *J Climate* (in press)
- Cohen J, Frei A, Rosen RD (2005) The role of boundary conditions in AMIP-II simulations of the NAO. *J Clim* 18:973–981
- Colman R, Deschamps L, Naughton M, Rikus L, Sulaiman A, Puri K, Roff G, Sun Z, Embery G (2005) BMRC Atmospheric Model (BAM) version 3.0: comparison with mean climatology. BMRC Research Report 108, 56pp
- Delworth TL (2006) GFDL's CM2 Global Coupled Climate Models. Part I: Formulation and simulation characteristics. *J Clim* 19(5):643–674
- Dong B, Sutton RT, Scaife AA (2006) Multidecadal Modulation of El Niño-Southern Oscillation (ENSO) variance by Atlantic Ocean sea surface temperatures. *Geophys Res Lett* 33:L08705
- Egorova T, Rozanov E, Zubov V, Manzini E, Schmutz W, Peter T (2005) Chemistry-climate model SOCOL: a validation of the present-day climatology. *Atmos Chem Phys* 5:1557–1576
- Folland CK, Parker DE, Palmer TN (1986) Sahel rainfall and worldwide sea surface temperature 1901–85. *Nature* 320:602–607
- Folland CK, Shukla J, Kinter J, Rodwell MJ (2002) The climate of the twentieth century project. *CLIVAR Exchanges* 7(2):37–39
- Frankignoul C, Hasselmann K (1977) Stochastic climate models. Part II: Application to sea-surface temperature anomalies and thermocline variability. *Tellus* 29:289–305
- Giannini A, Saravanan R, Chang P (2003) Oceanic forcing of Sahel rainfall on interannual to interdecadal time scales. *Science* 302:1027–1030
- Gordon HB, Rotstayn LD, McGregor JL, Dix MR, Kowalczyk AE, O'Farrell SP, Waterman AC, Hirst AC, Wilson MA, Collier IG, Watterson IG, Elliot TI (2002) The CSIRO Mk3 Climate System Model. Technical 60. CSIRO, Melbourne

- Hoerling MP, Hurrell JW, Xu T (2001) Tropical origins for recent North Atlantic Climate Change. *Science* 292: 90–92
- Hoerling MP, Hurrell JW, Xu T, Bates GT, Phillips AS (2004) Twentieth century North Atlantic climate change. Part II: Understanding the effect of Indian Ocean warming. *Clim Dyn* 23:391–405
- Huffman J et al. (1997) The Global Precipitation Climatology Project (GPCP) combined precipitation dataset. *Bull Am Met Soc* 78:5–20
- Hulme M (1994) Validation of large-scale precipitation fields in General Circulation Models. In: Debois M, Desalmand F (eds) *Global Precipitation and Climate Change*. NATO ASI series, vol 126. Springer, Heidelberg, pp 387–405
- Hurrell JW, Hoerling MP, Phillips AS, Xu T (2004) Twentieth century North Atlantic climate change. Part I: Assessing determinism. *Clim Dyn* 23(3–4):371–389
- Jones GS, Stott PA, Christidis N (2007) Human contribution to rapidly increasing frequency of very warm Northern Hemisphere summers. *J Geophys Res* (accepted)
- Knight JR, Folland CK, Scaife AA (2006) Climate impacts of the Atlantic Multidecadal oscillation. *Geophys Res Lett* 33:L17706
- Knutti R, Meehl GA, Allen MR, Stainforth DA (2006) Constraining climate sensitivity from the seasonal cycle in surface temperature. *J Clim* 19:4224–4233
- Kucharski F et al (2008) The CLIVAR C20C Project: Skill of simulating Indian monsoon rainfall on interannual to decadal timescales. Does GHG forcing play a role? *Clim Dyn* (in preparation)
- Kucharski F, Molteni F, Bracco A (2006) Decadal interactions between the Western Tropical Pacific and the North Atlantic Oscillation. *Clim Dyn* 26:79–91. doi:10.1007/s00382-005-0085-5
- Lau N-C, Nath MJ (2003) Atmosphere-ocean variations in the Indo-Pacific sector during ENSO episodes. *J Clim* 16:3–20
- Lee M-I, Kang I-S, Kim J-K, Mapes BE (2001) Influence of cloud-radiation interaction on simulating tropical intraseasonal oscillation with an atmospheric general circulation model. *J Geophys Res* 106:14219–14233
- Lee M-I, Kang I-S, Kim J-K, Mapes BE (2003) Impacts of cumulus convection parametrization on aqua-planet AGCM simulations of tropical intraseasonal variability. *J Meteor Soc Jap* 81:963–992
- Lorenz EN (1963) Deterministic nonperiodic flow. *J Atm Sci* 20:130–141
- Maloney ED, Chelton D (2006) An assessment of the sea surface temperature influence on surface wind stress in numerical weather prediction and climate models. *J Clim* 19:2743–2762
- Mehta VM, Suarez MJ, Manganello JV, Delworth TL (2000) Oceanic influence on the North Atlantic Oscillation and associated northern hemisphere climate variations: 1959–1993. *Geophys Res Lett* 27:121–124
- Minobe S, Kuwano-Yoshida A, Komori N, Xie S-P, Small RJ (2008) Influence of the gulf stream on the troposphere. *Nature* 452:206–210
- Murphy JM, Booth BBB, Collins M, Harris GR, Sexton DMH, Webb MJ (2007) A methodology for probabilistic predictions of regional climate change from perturbed physics ensembles. *Phil Trans Roy Soc A* 365: 1993–2028
- Nakamura M, Enomoto T, Yamane S (2005) A simulation study of the 2003 heatwave in Europe. *J Earth Sim* 2:55–69
- Namias J (1964) Seasonal persistence and recurrence of European blocking during 1958–60. *Tellus XVI*:394–407
- Palmer TN, Sun Z (1985) A modelling and observational study of the relationship between sea surface temperature in the north-west Atlantic and the atmospheric general circulation. *Quart J Roy Met Soc* 111: 947–975
- Pope VD, Gallani ML, Rowntree PR, Stratton RA, (2000) The impact of new physical parametrizations in the Hadley Centre climate model: HadAM3. *Clim Dyn* 16:123–146
- Ratcliffe RAS, Murray R (1970) New lag associations between North Atlantic sea temperatures and European pressure, applied to long range weather forecasting. *Quart J Roy Met Soc* 96:226–246
- Rayner NA, Parker DE, Horton EB, Folland CK, Alexander LV, Rowell DP, Kent EC, Kaplan A (2003) Global analyses of SST, sea ice, and night marine air temperature since the late nineteenth century. *J Geophys Res* 108(D14):4407. doi:10.1029/2002JD002670
- Rodwell MJ, Folland CK (2002) Atlantic air–sea interaction and seasonal predictability. *Q J R Met Soc* 128:1413–1443
- Rodwell MJ, Rowell DP, Folland CK (1999) Oceanic forcing of the winter North Atlantic Oscillation and European climate. *Nature* 398: 320–323
- Rodwell MJ, Drevillon M, gnoul C, Hurrell JW, Pohlmann H, Stendel M, Sutton RT (2004) North Atlantic forcing of climate. *Quart J R Meteorol Soc* 130:2013–2032
- Rowell DP (2003) The impact of Mediterranean SSTs on the Sahelian rainfall season. *J Clim* 16:849–862
- Rowell DP, Folland CK, Maskell K, Ward MN (1945) Variability of summer rainfall over tropical north Africa (1906–92): Observations and modelling. *Q J R Meteorol Soc* 121:669–704
- Saha S, Nadiga S, Thiaw C, Wang J, Wang W, Zhang Q, Van den Dool HM, Pan HL, Moorthi S, Bebringer D, Stokes D, Pena M, Lord S, White G, Ebisuzaki W, Peng P, Xie P (2006) The NCEP climate forecast system. *J Clim* 19:3483–3517
- Scaife AA, Knight JR, Vallis GK, Folland CK (2005) A stratospheric influence on the winter NAO and North Atlantic surface climate. *Geophys Res Lett* 32:L18715
- Schneider EK, Bengtsson L, Hu Z-Z (2003) Forcing of Northern Hemisphere climate trends. *J Atm Sci* 60:1504–1521
- Schraner M, Rozanov E, Schnadt C, Kenzelmann P, Fischer AM, Zubov V, Luo BP, Hoyle C, Füglistaler S, Egorova T, Brönnimann S, Peter T (2008) Chemistry-climate model SO-COL: version 2.0 with improved transport and chemistry/microphysics schemes. *Atmos Chem Phys* 8:11103–11147
- Schubert SD, Suarez MJ, Pegion PJ, Koster RD, Bacmeister JT (2004) On the cause of the 1930s Dust Bowl. *Science* 303:1855
- Sexton DMH, Rowell DP, Folland CK, Karoly DJ (2001) Detection of anthropogenic climate change using an atmospheric GCM. *Clim Dyn* 7:669–685
- Shibata K, Yoshimura H, Ohizumi M, Hosaka M, Sugi M (1999) A simulation of troposphere, stratosphere and mesosphere with an MRI/JMA98 GCM. *Papers Meteorol Geophys* 50:15–53
- Shneerov B.Ye., Meleshko VP, Matyugin VA, Sporyshev PV, Pavlova TV, Vavulin SV, Shkol'nik IM, Zubov VA, Gavrilina VM, Govorkova VA (2001) The up-to-date version of the MGO global model of general circulation of the atmosphere (version MGO-2). *MGO Proceedings*, No.550, pp 3–43
- Shukla J, DelSole T, Fennessy M, Kinter J, Paolino D (2006) Climate model fidelity and projections of climate change. *Geophys Res Lett* 33:L07702. doi:10.1029/2005GL025579
- Solomon S, Qin D, Manning M, Marquis M, Averyt K, Tignor MMB, Miller HL, Chen Z (eds) (2007) *Climate change 2007: the physical science basis*. Contribution of Working Group I to the Fourth Assessment Report of the Intergovernmental Panel on Climate Change. Cambridge University Press, Cambridge, pp 589–662
- Stenchikov G, Hamilton K, Stouffer RJ, Robock A, Ramaswamy V, Santer B, Graf H-F (2006) Arctic Oscillation response to volcanic eruptions in the IPCC AR4 climate models. *J Geophys Res* 111:D07107
- Stott PA, Kettleborough JA (2002) Origins and estimates of uncertainty in predictions of twenty-first century temperature rise. *Nature* 416: 723–726
- Thompson DWJ, Wallace JM, Hegerl GC (2000) Annular modes in the extratropical circulation. Part II. *Trends J Clim* 13:1018–1036

- Toniazzo T, Scaife AA (2006) The influence of ENSO on winter North Atlantic climate. *Geophys Res Lett* 33:L2704
- Trenberth KE, Caron JM, Stepanial DP, Worley S (2002) Evolution of El Nino-Southern Oscillation and global atmospheric surface temperatures. *J Geophys Res* 107. doi:[10.1029/2000JD000298](https://doi.org/10.1029/2000JD000298)
- Wang B, Wan H, Ji Z Z, Zhang X, Yu R C, Yu Y Q, Liu H L (2004) Design of a new dynamical core for global atmospheric models based on some efficient numerical methods. *Sci China (Ser A)* 47:4–21
- Zeng N, Neelin JD, Lau K-M, Tucker CJ (1999) Enhancement of interdecadal climate variability in the Sahel by vegetation interaction. *Science* 286: 1537–1540
- Zhang R, Delworth TL (2006) Impact of Atlantic multidecadal oscillations on India/Sahel rainfall and Atlantic hurricanes. *Geophys Res Lett* 33:L17702
- Zhou T et al (2008) The CLIVAR C20C Project: Which components of the Asian-Australian monsoon variability are forced and reproducible? *Clim Dyn* (in preparation)